Hindawi
Advances in Materials Science and Engineering
Volume 2018, Article ID 9692806, 7 pages
https://doi.org/10.1155/2018/9692806

Research Article

Heat Transfer Dynamic Analyses for Recycled-Concrete Wall Combined with Expanded Polystyrene Template

Jianhua Li and Wenjing Chen

Jiyang College, Zhejiang Agriculture and Forestry University, Shaoxing 311800, China

Correspondence should be addressed to Wenjing Chen; cwjing0703@163.com

Received 31 August 2017; Accepted 19 April 2018; Published 17 May 2018

Academic Editor: Fabrizio Pirri

Due to the benefits of pollution reduction, energy saving, and recycling of resources associated with the recycled concrete, together with the apparent thermal storage thermal insulation yield of expandable polystyrene (EPS) template, the heat transfer dynamics of their combination has become a contemporary study topic. In this research work, an investigation of the heat transfer coefficient (U) of EPS template recycled-concrete shear wall has been carried out. Four different concrete mixtures shear wall samples having different insulation types were developed for the purpose of quantifying their thermal outputs. Both temperature (T) and humidity (H) affection to thermal conductivity coefficient (λ) of reinforced concrete and the EPS template were investigated, correspondingly. The λ_0°C (relative variation for a 0°C of temperature variation in T) of cement mortar, recycled-concrete shear wall, and ordinary concrete shear wall were measured being 0.7526, 1.2463, and 1.3750 $W\cdot m^{-1}\cdot K^{-1}$, respectively. And the λ calculation of EPS was carried out being 0.0396 $W\cdot m^{-1}\cdot K^{-1}$. A corrected calculation method was put forward to application in practical work that could reflect the real U value in a more precise manner. These results brought to light the fact that the heat preservation output of recycled-concrete shear wall posed to be comparatively more improved than that of ordinary concrete shear wall. We put forth the suggestion for the use of corrected calculation method in the calculation and analysis of U of EPS template recycled-concrete composite shear wall in the climatic conditions of Beijing. The results revealed the fact that the U of EPS template recycled-concrete shear wall was dominantly controlled by the change of thermal conductivity changes of EPS template. The monthly mean U increased with increasing Tout and decreased with decreasing Tout. The smaller the U of the enclosure wall was, the better the thermal stability of the wall was experienced.

1. Introduction

The thermal storage as well as thermal insulation outputs of the external wall are expected to perform an essential function while developing energy preservation [1–3]. The thermal insulation output of the outer wall exerts a direct impact on the thermal insulating properties of the whole building, in addition to determining how much the heat flows in or out through the wall [4, 5]. Heat transfer coefficient (U) was typically put to use being an index for the measurement of the thermal storage as well as insulation output of enclosure wall. The better the thermal conservation together with thermal insulation output of retaining wall, the lesser the amount of heat flows through the wall and the smaller the energy consumed by air conditionings [6, 7].

Factors that regulate thermal conductivity coefficient (λ) are of interest to architects as well as construction engineers, owing to the fact that thermal preservation and insulation performance showcases a long standing discharge together with playing a quintessential function in building energy conservation and low carbon building in global C balance [8]. The study of building energy conservation asks for a comprehensive study of enclosure wall heat transfer. Thermal and humid atmospheres have been taken into consideration for affecting the output of enclosure wall heat shift [9]. The mass and energy conservation equation was employed for the purpose of analyzing as to how the environment of indoor and outdoor affects condensation, in specific, the tectonic pattern wall and heat flux through the wall. In their respective studies, the output of the

Table 1: Wall types and material properties.

Wall types	Layers	Thickness (mm)	Conductivity ($W{\cdot}m^{-1}{\cdot}k^{-1}$)	Density ($kg{\cdot}m^{-3}$)
ZDPJ1: Ord-Sam	Ordinary C40 concrete shear wall	130	1.740	2500
ZDPJ2: Rec-Sam	Recycled C40 concrete shear wall	130	1.540	2415
ZDPJ3: Uni-Sam	1 Cement grout	10	0.930	1800
	2 EPS template	56	0.038	29.50
	3 Recycled concrete shear wall	130	1.540	2415
ZDPJ4: Bil-Sam	1 Cement grout	10	0.930	1800
	2 EPS	56	0.038	29.50
	3 Recycled-concrete shear wall	130	1.540	2415
	4 EPS	56	0.038	29.50
	5 Cement grout	10	0.930	1800

considerable parameters was presumed not varied or the λ of materials were expressed as a constant [10, 11]. In addition, when expandable polystyrene (EPS) is employed for the purpose of thermal insulation, some results exhibit the best concrete slab thickness together with the thermal output of the composite shear wall [12, 13]. Nonetheless, there have been few measurements of heat transfer coefficient in the EPS template shear wall as well as the EPS recycled-concrete shear wall. To be specific, lack in the consideration of the physical parameters of material would change with environmental factors limiting the design refinement of EPS template recycled-concrete building energy conservation.

That is why there has been growing need of understanding the heat transfer coefficient of the EPS template recycled-concrete shear wall. Performance of empirical research was made for the purpose of comparing the impact of heat transfer coefficient on several sets of wall solutions. In this research work, there has been reported the findings of those tests that were carried out with the use of a climatic chamber in original service scenarios in Beijing background. The following are the key aims of this research: (1) conducting the test of the heat transfer coefficient (U) of EPS template recycled-concrete shear wall, (2) conducting the direct comparison of the thermal behavior of several builds of wall solutions, (3) putting to use the corrected computation method for the calculation as well as analysis of the EPS template recycled-concrete shear wall in Beijing for use.

2. Heat Transfer Coefficient Test and Theoretical Calculation

2.1. Types of Wall and Material Characteristics. There were developed four shear wall specimens, with one concrete shear wall and three recycled-concrete shear walls (Table 1). The cement put to use in all of them was Portland cement, featuring the compressive strength of >40 MPa following 28 days period. In accordance with the compressive strength grade, we defined sample 1 as ordinary C40 concrete shear wall (ZDPJ1) and sample 2–sample 4 as recycled C40 concrete shear walls (ZDPJ2-ZDPJ4). The coarse aggregate was ordinary gravel and 100% construction waste with the biggest diameter of 10 mm, correspondingly. Two different EPS insulation types were introduced to ZDPJ3 and ZDPJ4. A 56 mm thick EPS template was added unilaterally outside of ZDPJ3, together with two 56 mm thick EPS templates added bilaterally of ZDPJ4. All shear wall samples were designed with the same nominal water/cement ratio, that is, 0.37, and 1500 mm wide, 1500 mm high, and with different thicknesses. The details of the four samples are presented in Figure 1 and Table 1.

2.2. Test Apparatus. The experimental study was conducted with the help of steady-state heat transfer measurement apparatus (CD-WTFl515, Shenyang, China). Stimulation of the heat transfer scenario: the assayed building envelop is made at all seasons on the bases of single-directional steady heat transfer approach as well as the standard GB/T 13475-2008 [14] for the purpose of measuring and analyzing the heat transfer coefficient. Moreover, an environment control climate apparatus system comprises two air-conditioned chambers wherein temperature is brought under control by the help of heat resistance wires as well as refrigeration systems (Figures 2 and 3(a)). One chamber is put to use for the purpose of fake reproduction of external atmospheric climate wherein the metering tank temperature is fixed to be −10°C (having the allowable temperature variation of ±0.2°C). Application of the other chamber is made for the purpose of stimulating the internal atmosphere wherein the temperature is fixed at 35°C (having the allowable temperature variation of ±0.1°C). Developments of the EPS template of the recycled-concrete shear walls were done in accordance with the mass of the predetermined in the test instruments. The dimensions of the apparatus are 2600 mm in length, 2160 mm in width, and 2140 mm in height, correspondingly. The samples were made having the dimensions of 1500 mm in length, ≤400 mm in thickness, and 1500 mm in height, correspondingly (Figure 3(b)). Thereafter, the samples were treated through a natural dry processing for 28 days period. The interface between the test device and samples was sealed with polyurethane foams.

Making and testing of all of the specimens were done in Beijing building materials test center. Calibration of the apparatus is mandatory prior to putting the wall specimens into the testing apparatus. The indoor and external of the wall specimens are mandatorily required to be corresponded to the hot as well as cold chambers, correspondingly. Ten-minute calculations of specimen surface temperature were made with the help of the BD-WZP-PT100 temperature sensors (RTD, Shenzhen, China). Connections of 18 sample

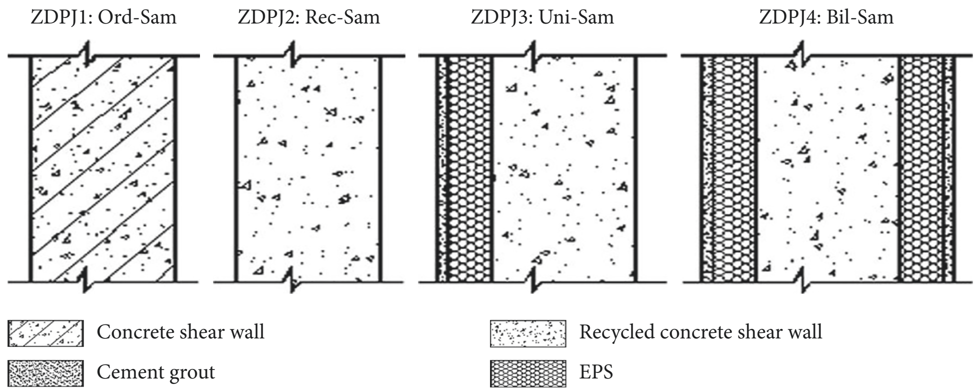

Figure 1: Four shear wall samples with different types.

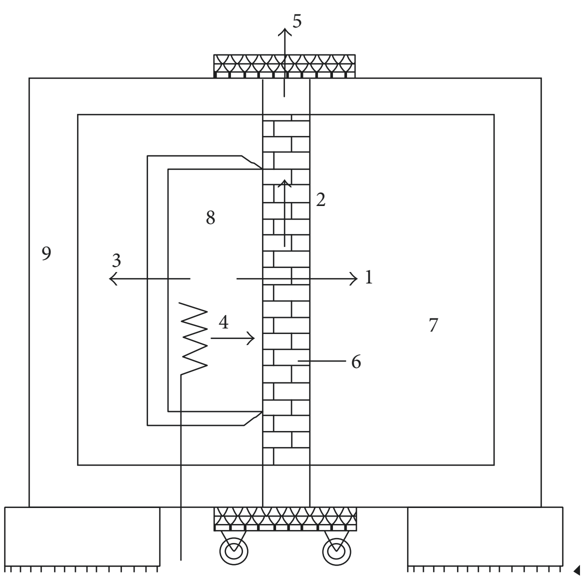

Figure 2: Environment control climate apparatus system. 1 refers to the heat flow through the samples; 2 refers to the uneven heat flow that is parallel to samples; 3 refers to the heat flow through the metering tank; 4 refers to the total input power; 5 refers to surrounding heat loss and the heat flow through the sample's boundaries; 6 refers to the sample; 7 refers to the cold chamber; 8 refers to the metering tank; 9 refers to the protective housing of the environment control climate apparatus.

surface temperature sensors were made on both facets of the respective positions of the specimens in a symmetrical manner, featuring a calculation precision of ±0.5°C. When the permissible temperature difference of the sample surface was within the range after 3 h of continuous climate control, the test was ended.

2.3. Heat Transfer Coefficient Calculation and Analysis

2.3.1. Test Value Measurement Rules. The test rule of steady-state heat transfer thermal output assaying equipment considered the bases of one-sided continuous heat shift. Furthermore, the specimens were placed between two varied temperature areas. The hot field and cold field simulated the indoor and outdoor air temperature, wind speed, and radiation, correspondingly. The device would achieve stable state subsequent to several hours of operations. Calculation of the heat flux through the metering box wall can be made with the application of the equation hereunder [12]:

$$Q_1 = M_1 \left(t_{\mathrm{is}} - t_{\mathrm{es}}\right), \tag{1}$$

where Q_1 suggests the heat flow through the metering box wall ($\mathrm{W{\cdot}m^{-2}}$), M_1 indicates the heat transfer coefficient of the metering wall ($\mathrm{W{\cdot}m^{-2}{\cdot}K^{-1}}$), t_{is} depicts the inner facade temperature of the metering box (K), and t_{es} implies the external façade temperature of the metering box (K).

Thereafter, calculation of the heat transfer coefficient of the enclosure structure can be made in accordance with the formula hereunder:

$$U_0 = \left(Q_{\mathrm{p}} - Q_1\right)\left[A\left(t_{\mathrm{ni}} - t_{\mathrm{ne}}\right)\right]^{-1}, \tag{2}$$

where Q_{p} suggests the aggregate power input ($\mathrm{W{\cdot}m^{-2}}$), A indicates the computed measurement filed that amounts to be $1.64\,\mathrm{m}^2$, t_{ni} suggests the temperature of the hot field (K), and t_{ne} implies temperature of the cold field (K).

2.3.2. The Theoretical Measurement Framework. The heat transfer coefficient is put to application for the purpose of measuring the thermal conservation output of building envelope. On the basis of the previous published empirical model [15], the computational expressions of heat transfer coefficient were

$$\begin{aligned} U_0 &= \left(R_{\mathrm{i}} + \sum R + R_{\mathrm{e}}\right)^{-1} = R_0^{-1}, \\ R &= d\lambda^{-1}, \end{aligned} \tag{3}$$

where U_0 implies the heat transfer coefficient of the building envelope ($\mathrm{W{\cdot}m^{-2}{\cdot}K^{-1}}$), R_{i} depicts the heat transfer resistance of the internal facade ($\mathrm{m^2{\cdot}K{\cdot}W^{-1}}$), R_{e} represents the heat transfer resistance of the external facade ($\mathrm{m^2{\cdot}K{\cdot}W^{-1}}$), R means the heat transfer resistance of each material ($\mathrm{m^2{\cdot}K{\cdot}W^{-1}}$), R_0 showcases the heat transfer resistance of the building envelope ($\mathrm{m^2{\cdot}K{\cdot}W^{-1}}$), d suggests the thickness of the materials (m), and λ indicates thermal conductivity coefficient of each material ($\mathrm{W{\cdot}m^{-1}{\cdot}K^{-1}}$).

2.4. Thermal Conductivity Coefficient Measurement under Original Working Atmosphere. The heat transfer coefficient

(a) (b)

Figure 3: The external view of the environment control climate apparatus (a), and the sample box (b).

of building envelope is primarily decided by the thermal conductivity coefficient of the materials. The thermal conductivity coefficient of each material was measured in accordance with the test standard with specified test methods. However, the thermal conductivity coefficient varied with environment temperature as well as humidity that gave birth to a divergence between the real value and hypothetical value. That is why there has been an increasing requirement of conducting the study of the real thermal conductivity coefficient of the material in varied atmospheres together with its extended implementation in energy preservation design.

2.4.1. Relationship between Thermal Conductivity Coefficient and Temperature. The models put to use for the description of the impacts of temperature on thermal conductivity coefficient of inorganic binding materials together with EPS templates were [16, 17]

$$\begin{aligned} \lambda_{t} &= 1.163\lambda_{0}{}^{\circ}\mathrm{C}(1+0.0025t), \\ \lambda_{\mathrm{EPS}} &= \lambda_{10}{}^{\circ}\mathrm{C}(0.9615+0.00399t), \end{aligned} \tag{4}$$

where λ_t suggests thermal conductivity coefficient of inorganic binding materials at mean temperature t, $\lambda_0{}^{\circ}$C represents the thermal conductivity coefficient at 0°C of temperature, t denotes the mean temperature of the material, λ_{EPS} indicates the thermal conductivity coefficient of EPS templates at mean temperature t, and $\lambda_{10}{}^{\circ}$C showcases the EPS thermal conductivity coefficient at 10°C of temperature.

2.4.2. Relationship between Thermal Conductivity Coefficient and Humidity. The influence of humidity on thermal conductivity coefficient of inorganic binding materials as well as EPS templates was fitted with linear regression analysis using these equations [14]:

$$\begin{aligned} \lambda_{\omega} &= \lambda\left[1+\left(1.163\omega_{\mathrm{V}}\delta_{\omega}\right)100^{-1}\right], \\ \omega_{\mathrm{V}} &= \omega_{\mathrm{g}}\rho\rho_{\mathrm{w}}^{-1}, \\ \delta_{\omega} &= 1.15_{\rho}^{2}-6.05\rho+14.3, \end{aligned} \tag{5}$$

where λ_{ω} suggests the moisture thermal conductivity coefficient, λ indicates the test value of the material thermal conductivity in natural drying scenarios, ω_{V} denotes the material moisture (%), ω_{g} represents the amount of condensation (kg), δ_{ω} indicates humidity corrected coefficient, ρ depicts the density of material (kg·m^{-3}), and ρ_{w} implies the density of water (kg·m^{-3}).

The influence of humidity on thermal conductivity coefficient of EPS template can be overlooked [18]. In the case that the walls showcase condensation mechanism, the daily quantity of condensation can be stated as follows:

$$\omega_{\mathrm{g}}' = 24\left[\left(P_{\mathrm{A}}-P_{\mathrm{s,c}}\right)H_{\mathrm{o,i}}^{-1}-\left(P_{\mathrm{s,c}}-P_{\mathrm{B}}\right)H_{\mathrm{o,e}}^{-1}\right], \tag{6}$$

where ω_{g}' indicates the everyday quantity of condensation (kg), P_{A} suggests the water vapor part pressure of higher partial pressure side (Pa), P_{B} depicts the water vapor part pressure of lower partial pressure dimension (Pa), $H_{\mathrm{o,i}}$ represents the water vapor permeability resistance of water vapor flowed in (m^2·h·Pa·kg^{-1}), and $H_{\mathrm{o,e}}$ reveals the water

Table 2: Comparison between measured values, theoretical values, and corrected computation values of wall heat transfer coefficient.

Number	$U_{experimental}$ ($W{\cdot}m^{-2}{\cdot}K^{-1}$)	$U_{theoretical}$ ($W{\cdot}m^{-2}{\cdot}K^{-1}$)	$U_{corrected}$ ($W{\cdot}m^{-2}{\cdot}K^{-1}$)
ZDPJ1	4.237	4.450	4.350
ZDPJ2	3.818	4.260	4.130
ZDPJ3	0.568	0.628	0.600
ZDPJ4	0.307	0.340	0.320

$U_{experimental}$ refers to the measured values of heat transfer coefficient. $U_{theoretical}$ refers to the theoretical values of heat transfer coefficient. $U_{corrected}$ refers to the corrected calculation values of heat transfer coefficient.

vapor permeability resistance of water vapor flowed out ($m^2{\cdot}h{\cdot}Pa{\cdot}kg^{-1}$).

3. Results

3.1. Thermal Conduction Coefficient Calculation and Simplifications. The heat transfer phenomenon of wall building materials possesses similarity with liquid that is to be dependent on elastic waves. Increase in the thermal conductivity was experienced with the increase in the temperature in addition to getting affected by humidity. Here, it is stated the overall equation in the scenario of real functioning scenario:

$$\begin{aligned}\lambda_{eff} &= \lambda + \Delta\lambda_t + \Delta\lambda'_\omega + \Delta\lambda''_\omega,\\ \Delta\lambda_t &= \lambda_t - \lambda,\\ \Delta\lambda'_\omega &= \lambda \times 1.163\omega_v\sigma_\omega/100,\end{aligned} \tag{7}$$

where λ suggests the test value of the material thermal conductivity, $\Delta\lambda_t$ depicts the thermal conductivity change brought forth by temperature, $\Delta\lambda'_\omega$ indicates the thermal conductivity change prompted by the weight humidity, and $\Delta\lambda''_\omega$ represents the thermal conductivity change aroused by frozen.

The thermal conductivity tests considered the bases of the cement mortar together with concrete thermal conductivity assay standards [19]. The thermal conductivity changes of the materials excited by the temperature and weight humidity in addition to getting frozen, thereafter, could be measured, correspondingly. The thermal conductivity (λ_0°C) (relative variation for a 0°C of temperature variation in T) of cement mortar, recycled-concrete shear wall, and ordinary concrete shear wall were measurement being 0.7526 $W{\cdot}m^{-1}{\cdot}K^{-1}$, 1.2463 $W{\cdot}m^{-1}{\cdot}K^{-1}$, and 1.3750 $W{\cdot}m^{-1}{\cdot}K^{-1}$, correspondingly. Furthermore, calculation of the EPS thermal conductivity coefficient (λ_{10}°C) was carried out being 0.0396 $W{\cdot}m^{-1}{\cdot}K^{-1}$.

3.2. Corrected Measurement of Heat Transfer Coefficient. Calculation of the heat transfer of building envelope was typically made on the bases of continuous heat transfer calculation in winter, whereby the thermal conductivities of materials posed to be the preset values [20]. Nonetheless, the thermal conductivity, featuring varied construction envelope materials together with structure kinds, though the changes are definitely dissimilar from continuous heat shift in real functioning scenario, has not conventionally been rectified in the backdrop of energy conservation research work. The corrected calculation procedure was delineated in detail in the literature [21]. The corrected calculation not only adhered to the equal law of energy preservation together with the heat flow density across the wall as well as each layer, but also satisfied proportional relationship between osmotic quantity and vapor pressure.

The temperature allocation within the wall, water vapor part pressure allocation, and water material were then calculated on the bases of the known values. The thermal conductivities of all of the contents were then modified for the purpose of calculating the heat transfer coefficient. A loop computation was carried out in order to recalculate the heat transfer coefficient until the value difference with the last measurement of heat transfer coefficient being within the prescribed scope.

3.3. Variations of the Experimental Value, Theoretical Value, and the Corrected Calculation Value. The empirical value, hypothetical value, and the rectified measurement value of U together with the measured thermal conductivity of ZDPJ2 were all lower than those of ZDPJ1 that expressed that the heat transfer impact of recycled-concrete posed to be superior to ordinary concrete (Table 2). While taking into consideration the impact of T as well as H variation, U of rectified measurement values appeared to be all lower than hypothetical values, in addition to being quite closer to the empirical values that could make it confirm that rectified measurement was accurate together with highlighting the heat transfer output in a precise manner.

The difference between experimental value, theoretical value, and the corrected calculation value of U got reduced on the addition of EPS template. U of ZDPJ3 was far less than ZDPJ2, suggesting that subsequent to the addition of 56 mm unilateral EPS template, the wall U apparently reduced, in addition to considerable increase in the energy conservation impacts. Nonetheless, U did not exhibit a continuous linear decrease with the thickness of the EPS template through the addition of bilateral EPS template but decreased gradually until its effects could be negligible. That is why while putting to use EPS template insulation, a reasonable thickness calculation was necessary in accordance with the actual environment.

4. Experimental Verification

The corrected computation method of U was followed for the purpose of calculating the monthly mean U of ZDPJ3 as well as ZDPJ4 in Beijing, with a constant temperature of 295 K, 50% relative humidity indoor, in addition to 10 years of monthly mean temperature, and relative humidity

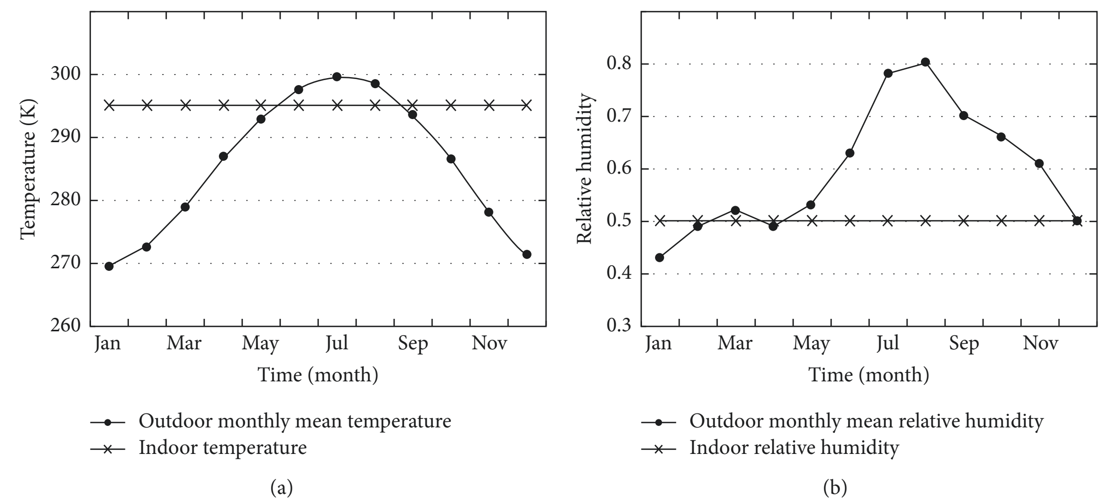

Figure 4: Ten years' monthly mean temperature outdoor with a constant indoor temperature of 295 K in Beijing (a), and ten years' relative humidity outdoor with 50% relative humidity indoor in Beijing (b).

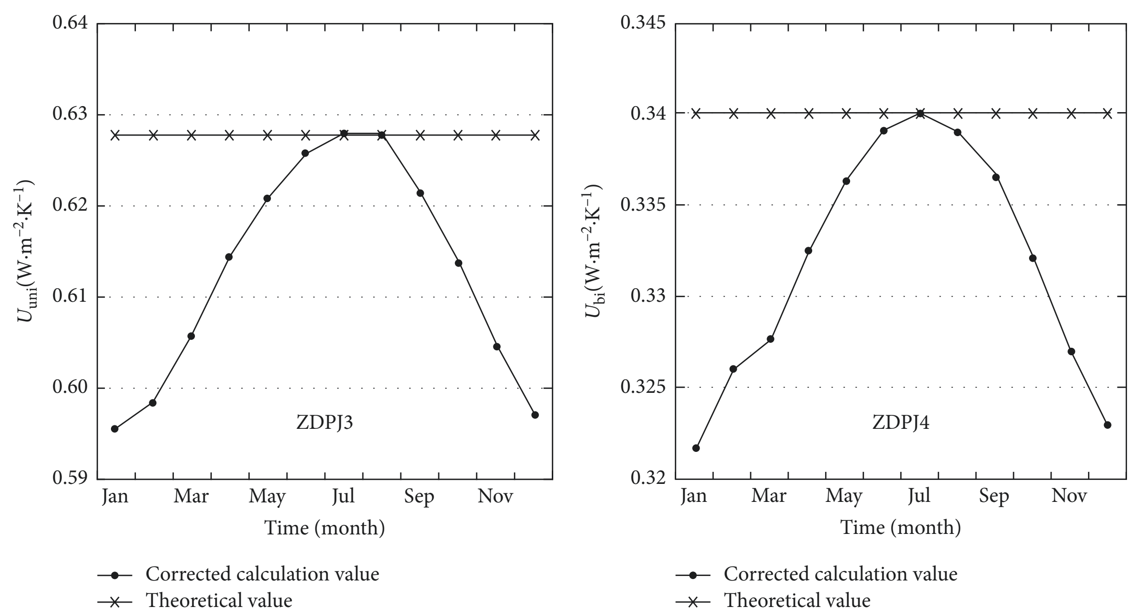

Figure 5: Comparing corrected computational method of monthly mean heat transfer coefficients (U) and theoretical values of ZDPJ3 and ZDPJ4.

outdoor in Beijing (Figure 4). The monthly mean U of ZDPJ3 brought a seasonal pattern to light that was quite same as that of T, showcasing increase in U with the setting in of the spring, getting at the top in the summers, and getting down all across the autumn season to the lowest level in the winter season.

The EPS thermal resistance accounted for 85% and 92% of the total thermal resistance of ZDPJ3 and ZDPJ4, correspondingly, that brought to light the fact that both the U of ZDPJ3 and ZDPJ4 were primarily dominated by EPS thermal conduction together with being strongly and significantly related to T (Figure 5). Nonetheless, the corrected U value of ZDPJ4 together with its range ability was always less than those of ZDPJ3 at the same time periods, depicting an improved thermal stability of the wall. To contract with the constant theoretical value of U, the use of revised U value could be able to more accurately highlight the wall heat transfer coefficient in addition to attaining a better energy saving effect.

5. Conclusions

In summary, the thermal conductivity coefficients' (λ) computational approaches of each material could be deduced in actual environment in accordance with the λ characteristics. The modified calculation method using dynamic changed λ substituted into heat transfer coefficients (U) calculation could reflect the regular pattern of wall heat transfer more rationally. Figure 5 brings forth the comparison of the corrected computational method of monthly mean U as well as theoretical values of ZDPJ3 and ZDPJ4 of different materials. With the help of the experiment comparisons, the U of recycled-concrete shear wall appeared to be less than that of normal concrete shear wall, reflecting a heat preservation performance enhancement together with a circular employing prospect of resource wall. U was primarily dominated by EPS thermal conduction in addition to being strongly and significantly associated with T. Meanwhile, U changed differently between adding unilateral EPS template and bilateral one and was not decreased linearly with the thickness of the EPS template.

Conflicts of Interest

The authors declare that they have no conflicts of interest.

Acknowledgments

This research was supported by grants from Talent Project of Jiyang College, Zhejiang Agriculture and Forestry University, China (JYRC201605, JYRC201604), and Ministry of Education Social Science Fund Project (14YJCZH113). The authors thank Beijing University of Technology of China for assistance with the testing instruments.

References

[1] S. Hou, F. Liu, S. Wang, and H. Bian, "Coupled heat and moisture transfer in hollow concrete block wall filled with compressed straw bricks," *Energy and Buildings*, vol. 135, pp. 74–84, 2017.

[2] V. Tyagi, A. Pandey, D. Buddhi, and R. Kothari, "Thermal performance assessment of encapsulated PCM based thermal management system to reduce peak energy demand in buildings," *Energy and Buildings*, vol. 117, pp. 44–52, 2016.

[3] P. Cao, B. Wu, and W. Liu, "Study on energy-saving technology of rural residential envelope structure in cold regions," *Advanced Materials Research*, vol. 830, pp. 411–415, 2014.

[4] F. Guarino, A. Athienitis, M. Cellura, and D. Bastien, "PCM thermal storage design in buildings: experimental studies and applications to solaria in cold climates," *Applied Energy*, vol. 185, pp. 95–106, 2017.

[5] A. La Rosa, A. Recca, A. Gagliano et al., "Environmental impacts and thermal insulation performance of innovative composite solutions for building applications," *Construction and Building Materials*, vol. 55, pp. 406–414, 2014.

[6] S. S. Chandel, V. Sharma, and B. Marwah, "Review of energy efficient features in vernacular architecture for improving indoor thermal comfort conditions," *Renewable and Sustainable Energy Reviews*, vol. 65, pp. 459–477, 2016.

[7] B. He, Y. Li, and M. Ye, "Building energy efficiency in China rural areas: Situation, drawbacks, challenges, corresponding measures and policies," *Sustainable Cities and Society*, vol. 11, pp. 7–15, 2014.

[8] H. Amecke, J. Deason, A. Hobbs, A. Novikova, Y. Xiu, and Z. Shengyuan, *Buildings Energy Efficiency in China, Germany, and the United States*, Climate Policy Initiative (CPI), London, UK, 2013.

[9] S. Shaik and A. Setty, "Influence of ambient air relative humidity and temperature on thermal properties and unsteady thermal response characteristics of laterite wall houses," *Building and Environment*, vol. 99, pp. 170–183, 2016.

[10] F. Kong and H. Wang, "Heat and mass coupled transfer combined with freezing process in building materials: modeling and experimental verification," *Energy and Buildings*, vol. 43, no. 10, pp. 2850–2859, 2011.

[11] Z. Pavlík and R. Černý, "Hygrothermal performance study of an innovative interior thermal insulation system," *Applied Thermal Engineering*, vol. 29, no. 10, pp. 1941–1946, 2009.

[12] T. Gao, "In-situ monolithically external concrete wall and external insulation board," *Construction Technology*, vol. 8, pp. 1–4, 2001.

[13] D. Peng, "CL wallboard concrete thickness analysis of hot summer and cold winter region," *Journal of Xi'an University of Science and Technology*, vol. 3, pp. 353–358, 2009.

[14] Standardization Administration of the People's Republic of China, *Thermal Insulation-Determination of Steady-State Thermal Transmission Properties-Calibrated and Guard Hot Box*, GB/T 13475-2008, China Standards Press, Beijing, China, 2008.

[15] Z. Chen, *Building Physics*, Vol. 12, Building Industry Press of China, Beijing, China, 2009.

[16] Q. Chen, *The Basis of Building Thermal Physical*, Xi'an JiaoTong University Press, Xi'an, China, 1991.

[17] I. Gnip, S. Vejelis, and S. Vaitkus, "Thermal conductivity of expanded polystyrene (EPS) at 100°C and its conversion to temperatures within interval from 0 to 500°C," *Energy and Buildings*, vol. 52, pp. 107–111, 2012.

[18] M. Jerman and R. Černý, "Effect of moisture content on heat and moisture transport and storage properties of thermal insulation materials," *Energy and Buildings*, vol. 53, pp. 39–46, 2012.

[19] JGJ134–2001, *Design Standard for Energy Efficiency of Residential Buildings in Hot Summer and Cold Winter Zone*, China Academy of Building Research, Beijing, China, 2001.

[20] Y. Xin, *Thermal Environment of Building*, Tsinghua University Press, Beijing, China, 1996.

[21] J. Li, W. Cao, and G. Chen, "The heat transfer coefficient of new construction—brick masonry with fly ash blocks," *Energy*, vol. 86, pp. 240–246, 2015.

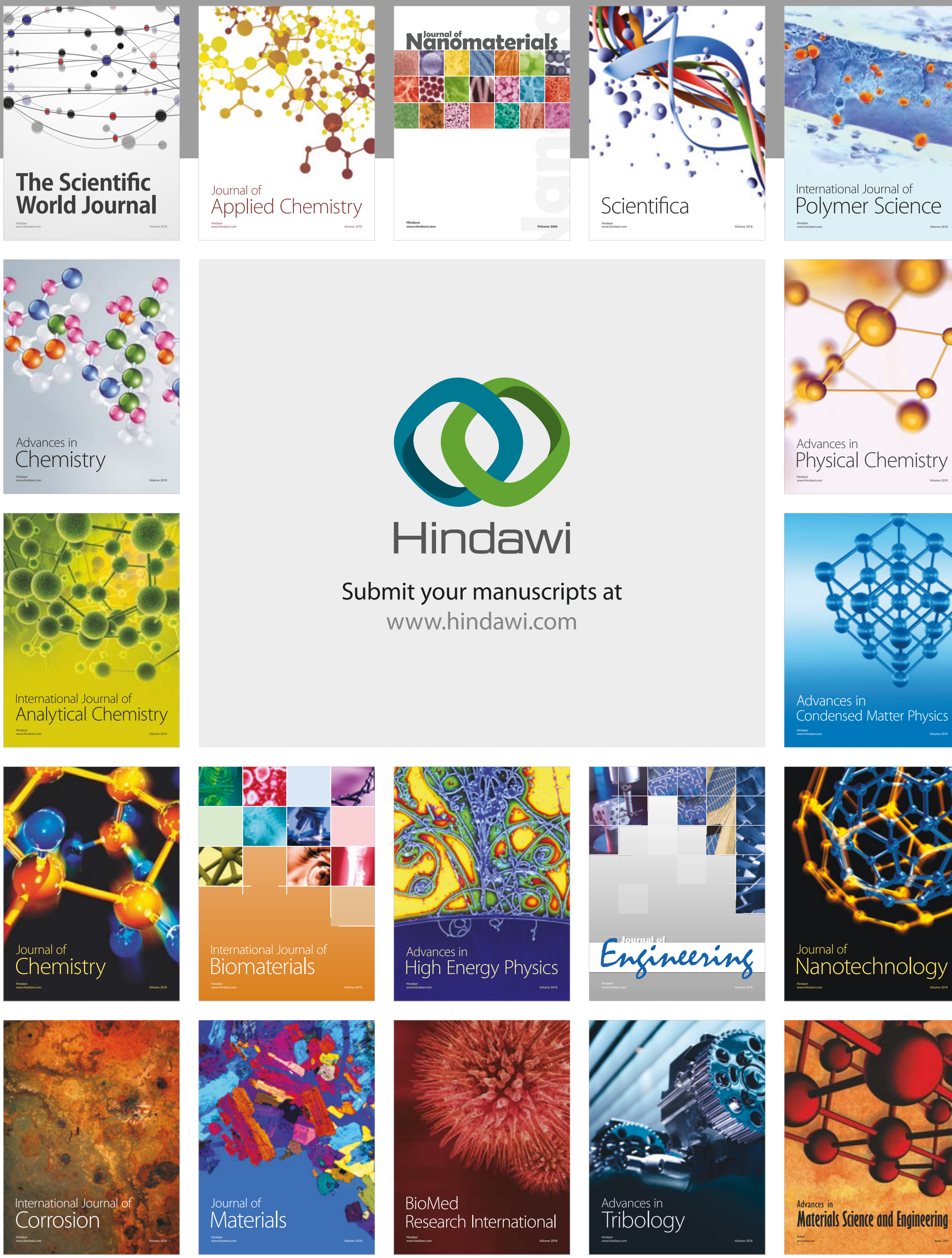

The Scientific World Journal
Journal of Applied Chemistry
Journal of Nanomaterials
Scientifica
International Journal of Polymer Science
Advances in Chemistry
Hindawi
Submit your manuscripts at
www.hindawi.com
Advances in Physical Chemistry
International Journal of Analytical Chemistry
Advances in Condensed Matter Physics
Journal of Chemistry
International Journal of Biomaterials
Advances in High Energy Physics
Journal of Engineering
Journal of Nanotechnology
International Journal of Corrosion
Journal of Materials
BioMed Research International
Advances in Tribology
Advances in Materials Science and Engineering